# A Novel Route to Octahedral $In_2O_3$ Particles Exhibiting Near Band Emission

Wu Zhang, Zhen Huang, Ting Li, Qun Tang, Dekun Ma, and Yitai Qian
*Hefei National Laboratory for Physical Sciences at Microscale and Department of Chemistry, University of Science and Technology of China, Hefei, Anhui 230026, P. R. China*

(Received September 29, 2004; CL-041147)

A novel solvothermal route combined with calcination was successfully established to synthesize octahedral $In_2O_3$ particles, which exhibit near band emission. Interesting shape transformation from amorphous sphere to well-shaped octahedron was found.

Inorganic nanoparticles with well-defined shapes are of special interest to understand basic size-dependent scaling laws and may be useful in a wide range of application fields, including photonics, nanoelectronics, information storage, catalysis, and biosensors. Recently, a series of well-shaped nanoparticles involving noble metals, oxides, and fluorides was successfully synthesized via different routes.[1–3]

Indium oxide is an important transparent conducting oxide (TCO) material that has wide applications in such as UV lasers, gas sensors, electrooptic modulators, low-emissivity windows, solar cells, flat-panel display, and electrochromic windows, because of its high electrical conductivity and high optical transparency.[4,5] Indium oxide also has very interesting superconductor–insulator transition behavior at low temperature and in low dimensions. In our previous work, $In_2O_3$ nanocubes truncated with {001} faces were synthesized by calcination of $In(OH)_3$ nanocubes.[6] Additionally, $In_2O_3$ nanoprisms were successfully produced via a selective epitaxial vapor–solid growth choosing the mixture of In and $In_2O_3$ powder as precursor.[7] Recently, on heating In chunks at 1200 °C, $In_2O_3$ octahedral particles were found.[8] By decomposing organometallic precursor, highly crystalline and size-controlled $In_2O_3$ nanoparticles were also prepared.[9,10] It can be deduced that different precursors have obvious influence on the final shape of products, which inspired us to explore a new unstable precursor to obtain nanoparticles with novel shapes. Thus, a new indium complex $In(cup)_3$ was chosen to be indium resource, octahedral $In_2O_3$ was achieved at 400 °C by calcination of amorphous indium oxide obtained by solvothermally decomposing the precursor.

In a typical procedure, 0.3 g of $In(cup)_3$ (prepared from $InCl_3$ and cupferron) was slowly added to 40 mL of benzene, the obtained solution was transferred into a stainless Teflon-lined 50-mL capacity autoclave, which was maintained at 220 °C for 24 h and then cooled to room temperature. The obtained products were washed with water and alcohol and dried at 60 °C for 4 h. The as-prepared products were heated in a boat crucible at a rate of 3 °C/min to 400 °C and maintained for 2 h in air. The morphology of the products was examined by field emission scanning electron microscopy (FESEM), performed on a JEOLJSM-6700F Scanning electron microanalyzer. The oriented growth direction and crystallinity can also be analyzed by X-ray diffraction measurement (Rigaku X-ray diffractometer with Cu K$\alpha$ radiation) and electron diffraction (Hitachi Model 800 at 200 kV). Photoluminescence spectrum was recorded on a Spex Fluorolog-3 spectrometer using an excitation of 250 nm with a 150-W Xe lamp at room temperature.

The XRD pattern of amorphous $In_2O_3$ was shown in Figure 1a, which is significantly different from XRD pattern of $In(cup)_3$. Figure 1b shows the XRD pattern of octahedral $In_2O_3$. All of the peaks can be indexed to a pure cubic phase [space group: *Ia*3] of $In_2O_3$ with lattice constant $a = 1.015$ nm, which is very consistent with the literature value of $a = 1.011$ nm (JCPDS 71-2195). The abnormally strong (222) refection suggested that the crystal might be truncated by {111} crystal face.

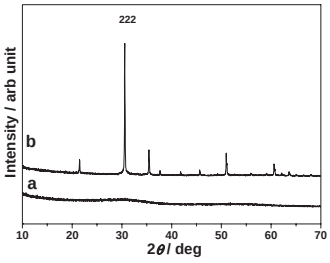


**Figure 1.** XRD pattern of (a) the amorphous $In_2O_3$; and (b) octahedral $In_2O_3$.

The typical SEM images of the amorphous $In_2O_3$ and octahedral $In_2O_3$ crystals are shown in Figures 2a and 2b. From Figure 2a, we can find that more than 90% particles of the as-obtained amorphous $In_2O_3$ are regular spheres with a mean diameter of 0.5–1.0 um. The calcined products are shaped as octahedrons with uniform side length, average value is about 500 nm as showed in Figure 2b, which has never reported as for $In_2O_3$ at relatively lower temperature. The octahedral structure of $In_2O_3$ was further examined with TEM image. The SAED pattern taken from a single octahedron can be exactly indexed to an $In_2O_3$ single crystal recorded from the [111] zone axis (insert in Figure 4d).

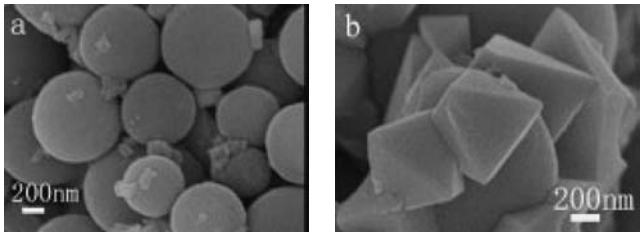


**Figure 2.** FESEM images of (a) the amorphous $In_2O_3$ sphere and (b) the octahedral $In_2O_3$.

Figure 3 shows a typical PL spectrum of high quality octahedral $In_2O_3$ measured at room temperature. It displays the emission maximum at 3.89 eV (318 nm) and blue-shifted 200 meV compared to the bulk 3.67 eV (338 nm), the emission can

be ascribed to NBE emission.[11] Furthermore, the products do not show PL emission at low energy (400–550 nm), which is always ascribed to amorphous $In_2O_3$ or oxygen vacancies.[12] In previous reference, ultrafine nanoparticle (<6 nm) will emit blue-shifted light by quantum effect.[6] In general, emission spectra can be divided into two broad categories: the near-band-edge (NBE) emissions and deep-level (DL) emissions. High crystal quality and the quantum confinement effect related to the nanostructures are two factors favoring the increase of the intensity of UV emission at room temperature.[11] Rather than quantum confinement effect, we attribute the shorter PL emission to the high crystal quality of $In_2O_3$ owing to the annealing process, which can decrease impurities and structure defects, such as oxygen vacancies. This leads to a high NBE emissions-to-DL-emissions ratio, which results in detectable UV emission at room temperature.

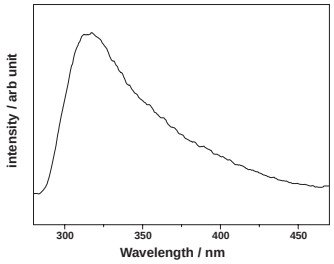


**Figure 3.** Photoluminescence spectrum of the octahedral $In_2O_3$.

The direct crystallization of amorphous precursors seems to be an alternative strategy to the templates or additives for the morphology control of inorganic substances.[13,14] As an unstable indium complex, $In(cup)_3$, can be easily decomposed under a relatively lower temperature, benzene-thermal treatment induced $In(cup)_3$ to decompose into amorphous $In_2O_3$ sphere, as showed in Figure 4a. Obviously, crystallization cannot be completed in such a low temperature. Further crystallization was carried out by calcination of the amorphous $In_2O_3$ sphere. The basic principle for the crystallization method is to control the crystallization kinetics of amorphous solids by optimizing the heat treatment conditions; the key to the formation of nanocrystallites in an amorphous solid is to control the calcination temperature such that the nucleation rate is high while the growth rate is slow. The calcinations temperature was determined by TG/DTA characterization. On the condition of low calcinations rate, an interesting shape transition was recorded by TEM image, as listed in Figures 4b–4d. In the initial period of calcination, some parts on the sphere extend out small corner, the corner is also well defined and some faces can be clearly detected in Figure 4b. As calcinations continued, sphere became smaller, the corners grew larger, and octahedron has been clearly differentiated, as shown in Figure 4c. Finally, the sphere completely disappeared and transformed into regular octahedron when calcination was maintained for 2 h (Figure 4d). However, on the condition of high calcinations rate, no regular shape was found in the final calcined product.

As for our designed procedure, amorphous $In_2O_3$ sphere dissolved gradually and supplied enough nutrition for the growth of the well-defined particle. It is well known that most of the amorphous particles have a strong transformation tendency from thermodynamics metastable state to stable crystalline state under appropriate conditions. Furthermore, the crystallization is generally accompanied with the formation of desired structure due to the necessity to obtain a match between the symmetry of the crystal and their geometric shape.

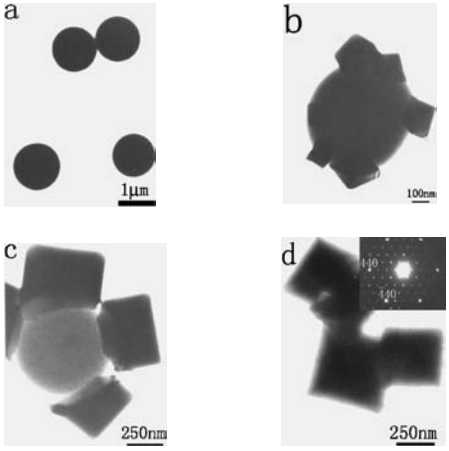


**Figure 4.** Development of $In_2O_3$ octahedral nanoparticle recorded by TEM images.

In summary, by a designed two-step route octahedral $In_2O_3$ nanoparticles were successfully synthesized at relatively low temperature. PL spectra showed the as-obtained $In_2O_3$ are highly crystalline and defect-free, which is beneficial for its application in optic and electronic devices.

Financial support from the National Nature Science Fund of China and the 973 Project of China are appreciated.

## References

1 Y. G. Sun and Y. N. Xia, *Science*, **298**, 2176 (2002).
2 L. F. Gou and C. J. Murphy, *Nano Lett.*, **3**, 231 (2003).
3 X. M. Sun and Y. D. Li, *Chem. Commun.*, **2003**, 1768.
4 K. G. Gopchandran, B. Joseph, J. T. Abaham, P. Koshy, and V. K. Vaidyan, *Vacuum*, **48**, 547 (1997).
5 R. G. Gordon, *MRS Bull.*, **2000**, 52.
6 Q. Tang, W. J. Zhou, W. Zhang, S. M. Ou, K. Jiang, W. C. Yu, and Y. T. Qian, *Cryst. Growth Des.*, accepted.
7 Y. Zhang, H. B. Jia, D. P. Yu, X. H. Luo, Z. S. Zhang, X. H. Chen, and C. Lee, *J. Mater. Res.*, **18**, 2793 (2003).
8 Y. J. Zhang, H. Ago, J. Liu, M. Yumura, K. Uchida, S. Ohshima, S. Iijima, J. Zhu, and X. Z. Zhang, *J. Cryst. Growth*, **264**, 363 (2004).
9 W. S Seo, H. H. Jo, K. Lee, and J. T. Park, *Adv. Mater.*, **15**, 795 (2003).
10 K. Soulantica, L. Erades, M. Sauvan, F. Senocq, A. Maisonnat, and B. Chaudret, *Adv. Funct. Mater.*, **13**, 553 (2003).
11 H. Q. Cao, X. Q. Qiu, Y. Liang, and Q. M. Zhu, *Appl. Phys. Lett.*, **83**, 761 (2003).
12 H. J. Zhou, W. P. Cai, and L. D. Zhang, *Appl. Phys. Lett.*, **75**, 495 (1999).
13 Z. Y. Tang, N. A. Kotov, and M. Giersig, *Science*, **297**, 237 (2002).
14 K. Lu, *Adv. Mater.*, **11**, 1127 (1999).

Published on the web (Advance View) December 22, 2004; DOI 10.1246/cl.2005.118